J Mater Sci: Mater Med (2009) 20:507–512
DOI 10.1007/s10856-008-3592-1

Study of mesoporous silica/magnetite systems in drug controlled release

K. C. Souza · J. D. Ardisson · E. M. B. Sousa

Received: 8 July 2008 / Accepted: 8 September 2008 / Published online: 7 October 2008

Abstract Ordered mesoporous materials like SBA-15 have a network of channels and pores with well-defined size in the nanoscale range. This particular silica matrix pore architecture makes them suitable for hosting a broad variety of compounds in very promising materials in a range of applications, including drug release magnetic carriers. In this work, magnetic nanoparticles embedded into mesoporous silica were prepared in two steps: first, magnetite was synthesized by oxidation–precipitation method, and next, the magnetic nanoparticles were coated with mesoporous silica by using nonionic block copolymer surfactants as structure-directing agents. The materials were characterized by X-ray diffraction (XRD), Fourier-transform infrared spectroscopy (FTIR), N_2 adsorption, and scanning electron microscopy (SEM). The influence of magnetic nanoparticles on drug release kinetics was studied with cisplatin, carboplatin, and atenolol under in vitro conditions in the absence and in the presence of an external magnetic field (0.25 T) by using NdFeB permanent magnet. The constant external magnetic field did not affect drug release significantly. The low-frequency alternating magnetic field had a large influence on the cisplatin release profile.

K. C. Souza · J. D. Ardisson · E. M. B. Sousa (✉)
Centro de Desenvolvimento da Tecnologia Nuclear—CDTN/CNEN, Belo Horizonte, Minas Gerais 30123-970, Brazil
e-mail: sousaem@cdtn.br

K. C. Souza
Departamento de Química, UFMG, Belo Horizonte, Minas Gerais, Brazil

1 Introduction

Controlled drug release systems are a major scientific application of biomaterials. The potential advantages of controlled drug release systems include drug delivery targeted at particular body parts with reduced drug levels and the preservation of drugs that otherwise would be rapidly destroyed by the body. This is particularly important for biologically sensitive molecules such as proteins [1].

Polymeric materials generally release drugs by the following mechanisms: (i) diffusion, (ii) chemical reaction, or (iii) solvent activation. Furthermore, some polymer systems can be externally activated to release more drugs when necessary, such as through the use of external forces like magnetism. In these systems, magnetic nanoparticles are uniformly dispersed within the polymer and when they are exposed to a biological system, normal diffusion of the drug occurs due to concentration gradient. However, upon exposure to an external alternating magnetic field, large quantities of drug can be quickly released [2].

The use of a magnetic matrix as a carrier of a specific drug is very interesting. The high surface area of the nanoparticles may influence the material performance and biocompatibility in biological environments. The particles must remain nonaggregated, be stable against oxidation, and display high magnetization during application. Transition metals offer high magnetization, but they are sensitive to oxidation. Currently, the oxidization of transition metals remains a hurdle, especially in biomedical, oxygen-rich environments. Iron oxides like magnetite (Fe_3O_4) and maghemite (γ-Fe_2O_3) are more stable against oxidation [3]. Thus, coating nanoparticles appropriately is essential to overcome this limitation. Silica/magnetite nanocomposites are particularly interesting, since the protective layer afforded by silica can prevent the dipolar

magnetic attraction between magnetite particles, and consequently, afford rather uniform particle dispersion.

Nanocomposites of magnetic phases in the form of nanoparticles combined with mesoporous materials like SBA-15, can be coated with an open pore structure and isolated from each other to prevent their aggregation and degradation. SBA-15 has a homogeneous distribution of mesopores of around 6 nm and very narrow pore size distribution [4–6]. The pore size and volume of these materials make them suitable as potential matrices for hosting and the release of a large variety of molecules with therapeutic activity [7–10].

The synthesis of a mesostructured silica/magnetite nanocomposite appears to be an attractive alternative in the study of drug release systems with bioactive characteristics and the controlled drug release under an external alternating magnetic field. In this work, the performance of the system SBA-15/Fe_3O_4 in the release of anticancer drugs like cisplatin and carboplatin was evaluated and compared with that of a beta-blocker drug standard, atenolol. The influence of the magnetic nanoparticles on the drug release kinetics with and without external magnetic field has been investigated.

2 Materials and methods

2.1 Synthesis of materials

Magnetite nanoparticles were synthesized by crystallization from ferrous hydroxide gels based on the methodology proposed by Sugimoto and Matijevic [11]. Solutions of potassium hydroxide, iron (II) sulphate heptahydrate, and potassium nitrate were prepared. The reaction mixture was heated to 90°C under N_2 and maintained at this temperature for 2 h. A black precipitate was formed. After cooling, the precipitate was washed using magnetic sedimentation of the solid with the aid of a slab magnet. Next, the nanoparticles were dried in vacuum at 45°C for 48 h.

The SBA-15/Fe_3O_4 nanocomposite (40 wt% Fe_3O_4) was obtained according to the method reported by Souza [9]. Following the route to prepare pure SBA-15, after dissolution of the surfactant in deionized water and in acidic environment (37% solution), the previously synthesized magnetite was added to the solution, followed by the silica precursor, tetraethyl orthosilicate (TEOS). The solution was stirred for 24 h at constant temperature of 37°C. After aging under continuous stirring at 100°C in a hermetically closed Teflon® recipient for 24 h, the solids were collected by filtration and dried in air at 40°C. The surfactant was removed by calcination at increasing temperature up to 550°C under N_2 flow.

2.2 Characterization

The samples were characterized by X-ray diffraction (XRD), Fourier-transform infrared spectroscopy (FTIR), and scanning electron microscope (SEM). Low-angle XRD measurements were obtained using synchrotron radiation with wavelength $\lambda = 1.5494$ nm. Synchrotron radiation measurements were carried out at the D10A-XRD2 beam line of LNLS (Campinas, Brazil) using a Huber-423 three-circle diffractometer. The high-angle XRD patterns were obtained using a Rigaku Geigerflex-3034 diffractometer with a Cu Kα tube. Specific surface area and pore size distribution were determined by N_2 adsorption using the BET and BJH methods, respectively, in an Autosorb–Quantachrome Nova 1200. The samples were outgassed for 2 h at 300°C before analysis. FTIR measurements were conducted with a PerkinElmer 1760-X spectrophotometer in the range 4,000–400 cm^{-1}. The FTIR spectra were recorded at room temperature using KBr pellets. The SEM images were obtained in JEOL JSM, model 840A with secondary electron.

2.3 Drug release assays

In vitro drugs release assays were performed as follows: previously calcined powders were conformed into 0.10 g disks by uniaxial pressure (1.5 MPa). The drug release profiles were obtained by soaking the disks in 30 ml of simulated body fluid (SBF) at 37°C under stirring. UV spectrometry (UV–Vis Shimadzu, model 2401) was used to monitor the amounts of drug released as a function of time. The drug concentration in SBF was found from the intensity of the absorption bands at 274 nm (atenolol), 212 nm (cisplatin), and 231.7 nm (carboplatin). Drug release was studied with and without magnetic field in two experiments: (a) with constant magnetic field and (b) with alternating magnetic field. To simulate drug release in the presence of a magnetic field, a NdFeB magnet (0.250 T) was used in the first experiment, and in the second one, a low-frequency alternating magnetic field was obtained with a magnetic cavity composed of a Helmholtz coil connected to a direct current source coupled to a frequency generator and a Hall probe for measuring the magnetic field. The following frequencies were used: 15, 30, 45, 60, 100, and 300 Hz with a 17 mT magnetic field. The measurement maximum error was 10%.

3 Results and discussion

XRD patterns of pure magnetite, pure mesoporous silica, and the nanocomposites are shown in Fig. 1a. All the observed diffraction peaks can be indexed to the spinel

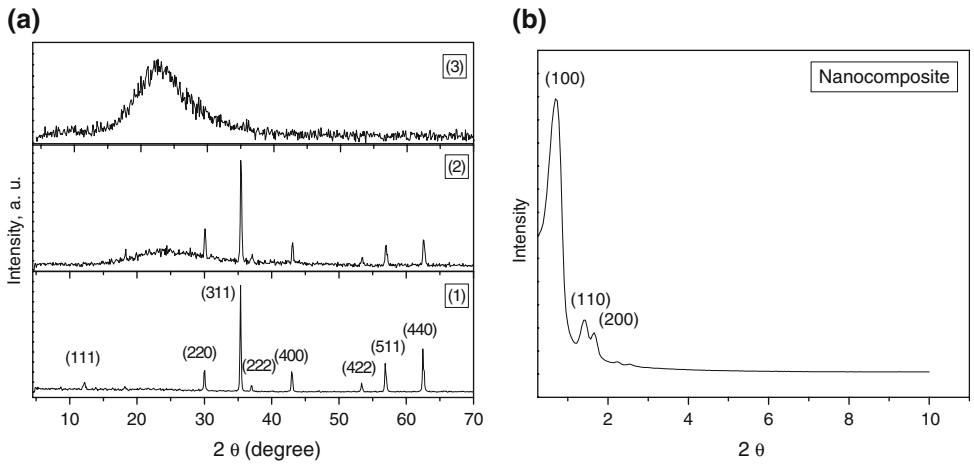

Fig. 1 (**a**) XRD patterns of Fe_3O_4 (1), SBA-15/Fe_3O_4 (2), and pure SBA-15 (3) samples, and (**b**) SAXRD of SBA-15/Fe_3O_4 nanocomposite

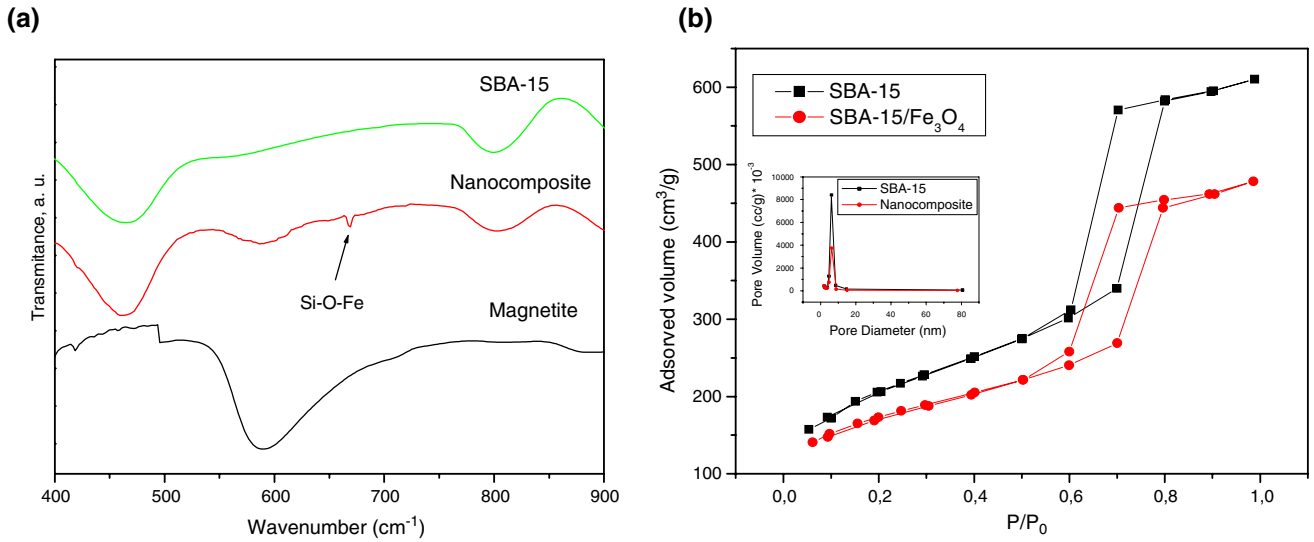

Fig. 2 (**a**) FTIR spectra and (**b**) N_2 adsorption isotherms and pore size distribution of pure SBA-15 and SBA-15/Fe_3O_4 nanocomposite

structure of pure stoichiometric magnetite (Fe_3O_4) (JCPDS file 19-0629). The amorphous region between ca. 15° and 30° corresponds to the amorphous silica matrix, Fig. 1a3. Small-angle X-ray reflection diffractometry (SAXRD) data of the SBA-15/Fe_3O_4 nanocomposite are presented in Fig. 1b. It shows typical peaks of a well-organized pore structure material with the main reflection in 2θ at 0.89° and other low intensity reflections at 1.6° and 1.7°. Three diffraction planes were found, (100), (110), and (200), which shows a well ordered hexagonal lattice. Mössbauer spectroscopy indicated that the magnetite was conserved during the synthesis of the nanocomposites [9].

Figure 2a shows the FTIR spectra of pure SBA-15 and the SBA-15/Fe_3O_4 nanocomposite. The spectrum of SBA-15 shows typical silica peaks with relatives bands of Si–O–Si bonds (1,080 and 1,160 cm^{-1}), Si–O (810 and 460 cm^{-1}), and Si–OH (960 cm^{-1}), which are characteristic of mesoporous silica. An additional peak (660 cm^{-1}) is observed in the spectrum of the magnetic nanocomposite sample. According to Choi et al.[12], this peak may be due to the formation of metal–oxygen–silicon bonds (Si–O–Fe) in the structure of mesoporous silica.

Figure 2b shows the N_2 adsorption isotherms of the SBA-15 and SBA-15/Fe_3O_4 samples and Table 1 summarizes these results. The samples exhibit type IV isotherms

Table 1 N_2 adsorption

Sample	S_{BET} (m^2/g)	D_p (nm)	V_p (cm^3/g) × 10^{-3}
SBA-15	789	6.2	1.329
Fe_3O_4	4	11.7	0.010
SBA-15/Fe_3O_4	585	6.2	0.739

S_{BET} = Specific area; D_p = Mean pore diameter; V_p = Mean pore volume

Related error: 3%

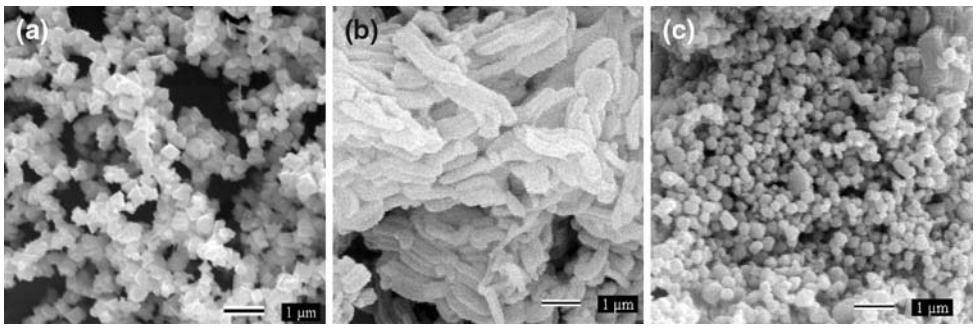

Fig. 3 SEM of (**a**) magnetite, (**b**) pure SBA-15, and (**c**) SBA-15/Fe_3O_4

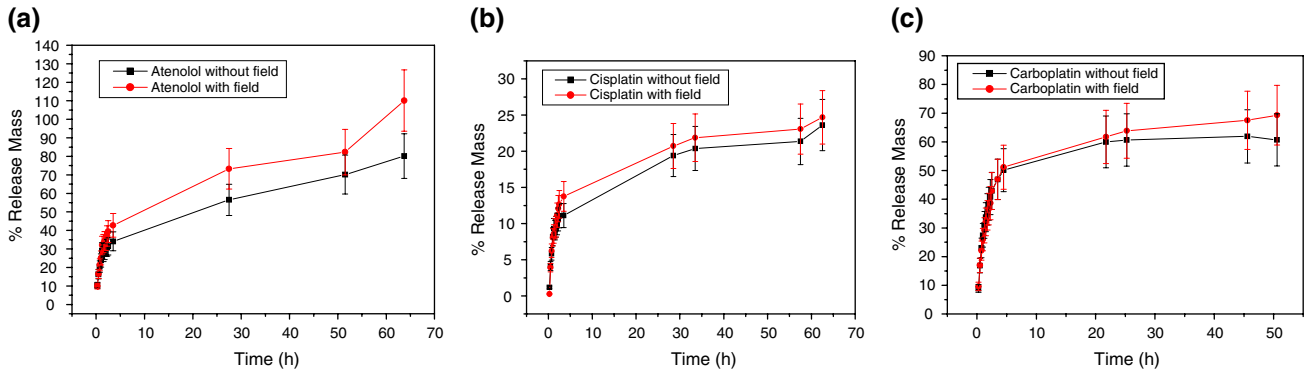

Fig. 4 Atenolol (**a**), cisplatin (**b**), and (**c**) carboplatin mass release from nanocomposites with and without the influence of an external magnetic field

and a typical adsorption isotherm with H1 hysteresis, according to the IUPAC classification, associated with the presence of mesopores. The p/p_0 position of the inflection range from 0.6 to 0.8 confirms this structural (porous) characteristic and the sharpness of the step indicates the uniformity of the mesopore size distribution. For the nanocomposite, the overall adsorption of N_2 decreased at all relative pressures; however, the pore size was not affected by the presence of Fe_3O_4.

The samples presented a narrow pore size distribution by the BJH method, as shown by the insert in Fig. 2b. The pure SBA-15 and the nanocomposite have similar pore size distributions centered at 6 nm (D_p), which is typical of mesoporous materials with well-ordered structure. The adsorption isotherm and pore size distribution results show that the iron nanoparticles occupy the mesopore free space intrachannels only partially. This makes this composite a promising candidate for the incorporation and subsequent release of a variety of pharmaceutical molecules under appropriate conditions.

The SEM images of magnetite in Fig. 3 show that the material has uniform morphology and particle size distribution. In addition, some particle clusters may be observed due to the magnetic interaction between the particles. The regular octahedral morphology indicates that the particles are well crystallized. Figure 3b shows the morphology of SBA-15. It consists of vermicular-shaped particles, as described by Zhao et al.[13]. In contrast, the nanocomposite presents spherical morphology. This may be attributed to the presence of the magnetite silica-coated nanoparticles. The average size of the spherical particles varied from 0.139 to 0.476 μm according to Quantikov Image Analyzer software [14]. Particles smaller than the human body capillary diameter (8 μm) [15] are suitable for intravenous drug-delivery injection. The desired particle size range for a specific application may be selected by nanoparticle centrifugation at a controlled rate.

The release kinetics of different drugs was studied as a function of time. The results for the SBA-15/Fe_3O_4 systems under magnetic field of 0.25 T applied with a NdFeB magnet are shown in Fig. 4.

The external magnetic field did not influence drug release by any of the systems. After 10-h assay, the release rate increased slightly, reaching 3% for cisplatin and 12% for atenolol. However, the carboplatin system showed an increase of only 2% for the same time. After about 24 h of experiment, the difference in the release of cisplatin dropped to 2%, while that of carboplatin increased to 4%, and that of atenolol increased to 15%.

In order to investigate the influence of the nanocomposite structure and the magnetic field on the release of the various drugs, the results were analyzed according to the Higuchi model [16]. The mechanisms of release by this system consider the drug leaching to the bath fluid, which can enter the drug-matrix phase through the pores. The drug is presumed to dissolve slowly into the fluid phase and

diffuse from the system along the solvent-filled capillary channels. According to Higuchi [16], for release from a planar system with a porous matrix, Eq. 1 may be used to fit the drug release rates:

$$Mt = Kt^{1/2} \quad (1)$$

where M is the overall amount of drug released after time t and K is a release constant.

In general, the diffusion-controlled drug release from matrix-type drug release systems has a linear relationship with small deviations from linearity for all matrices. The K values were estimated by using the square root of time. The application of the Higuchi model follows some postulates: (a) the initial concentration of the substance in the system must be higher than its solubility in the medium, (b) the mathematical analysis is based on one-dimensional diffusion, (c) the substance is considered in a molecularly disperse state with particles much smaller in diameter than the thickness of the system, (d) the dissolution of the matrix carrier is negligible, and (e) the diffusibility of the substance is constant.

To simplify the analysis of data of systems with various geometries, in the Korsmeyer-Peppas model [17], an empirical exponential expression is used to relate drug release with fractional release time (Eq. 2):

$$M_t/M_\infty = Kt^n \quad (2)$$

where M_t/M_∞ is the fractional solute release, t is the release time, K is a constant, and n is the diffusional exponent characteristic of the release mechanism. The parameters of Eq. 2 can be obtained from Eq. 3:

$$\ln(M_t/M_\infty) = \ln K + \mathrm{n} \ln t \quad (3)$$

In cases of pure Fickian release, exponent n has the limiting values of 0.5, 0.45, and 0.43 for release from slabs, cylinders, and spheres, respectively. For tablets, and depending on the diameter-thickness ratio, the Fickian diffusion mechanism is described by $0.43 < n < 0.50$. For drug release from spherical particles with wide size distribution, the value of n for Fickian diffusion depends on the distribution width [18, 19]. Table 2 presents the kinetics study results for nanocomposite/drug systems with and without external magnetic field. It is observed that n is lower than 0.5, which may be explained by the small variation of the agglomerate size of the nanocomposite particulate phase covered by silica, as shown in Fig. 3c. This leads to a decrease in n, as described by Ritger and Peppas [19]. They studied the effect of particle size distribution on drug release kinetics. In comparison to the release behavior of a monodisperse sample, the particle size distribution causes a substantial acceleration of transport at early stages and marked transport delay for long release times. The acceleration of the early portion of the release curve results from the release from particles smaller than the mean particle size. Particles larger than the mean particle size delay transport at long times. For a Fickian diffusion process, $n = 0.30 \pm 0.01$, which is different from the value of n obtained for the release from a monodispersed sample, i.e., $n = 0.43$. The K values presented in Table 2 show that the magnetic field affects the system release to a small extent, especially for platinum-based drugs.

Table 2 Kinetics parameters of different systems with and without magnetic field

Systems	n	r	K	Kinetics mechanisms
Cisplatin without field	0.29	0.96	7	Fickian diffusion
Cisplatin with field	0.30	0.94	8	Fickian diffusion
Carboplatin without field	0.25	0.90	27	Fickian diffusion
Carboplatin with field	0.26	0.94	28	Fickian diffusion
Atenolol without field	0.32	0.98	22	Fickian diffusion
Atenolol with field	0.32	0.97	26	Fickian diffusion

As the drug release was little influenced by the constant magnetic field, we investigated the influence of a low-frequency alternating magnetic field on the release of cisplatin, the studied drug with the lowest release rate. The study was based on the model proposed by Dash and Cudworth [2], in which the application of an alternating magnetic field provokes the vibration of the magnetic particles and the quick release of large quantities of drugs. The measures presented here are designed to assess the influence of the application of low frequency ($\leq$300 Hz) alternating magnetic fields (170 Oe) on drug release. Figure 5a shows the release profiles of cisplatin without magnetic field, with constant magnetic field, and alternating magnetic field up to 300 Hz. Drug release was more effective and faster in alternating magnetic field.

Table 3 presents the kinetics results for the release of cisplatin from the nanocomposite. The values of n show under alternating magnetic field, the mechanism of release of cisplatin changes from Fickian to zero order. This mechanism is related to the quick release of the drug from the matrix.

4 Conclusion

The synthesized nanocomposites presented a well-ordered mesoporous structure described as hexagonal mesopores separated by a wall of continuous silica layer coating the magnetic particles. According to XRD data, magnetite was preserved during the synthesis of the nanocomposite. SEM data showed that the silica network coated the magnetite particles. The nanoparticle mean size was 138 nm. The constant external magnetic field did not affect drug release

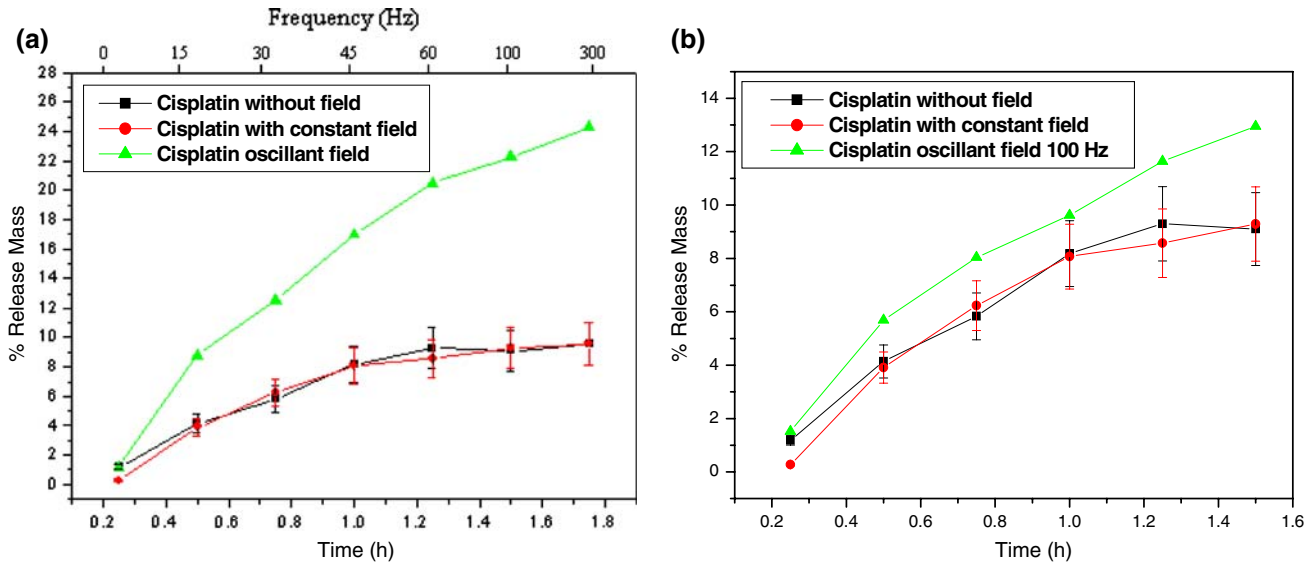

Fig. 5 (**a**) Release profile of the nanocomposite/cisplatin system without field, in constant field, and in alternating field, (**b**) 100-Hz constant field and alternating field (single measurement)

Table 3 Kinetics parameters of the different systems with and without constant and varying magnetic field

Systems	*n*	*r*	*K*	Kinetics mechanisms
Cisplatin without magnetic field	0.29	0.96	7	Fickian diffusion
Cisplatin with magnetic field	0.30	0.94	8	Fickian diffusion
Cisplatin with varying alternating magnetic field	0.91	0.98	19	Zero order
Cisplatin with 100-Hz alternating magnetic field	1.16	0.97	10	Zero order

significantly. The low-frequency alternating magnetic field had a large influence on the cisplatin release profile. These results can be explained by the possible interaction of the drugs with the magnetite nanoparticles, possibly due to the incorporation of cisplatin into the mesopores and its interaction with the surface of the magnetic nanoparticles.

Acknowledgments The authors are grateful to CAPES, CNPq, FAPEMIG, and LNLS (Campinas—Brazil) for supporting this work.

References

1. R. Langer, Science **249**, 1527–1533 (1990). doi:10.1126/science.2218494
2. A.K. Dash, G.C. Cudworth, J. Pharmacol. Toxicol. Methods **40**, 1 (1998). doi:10.1016/S1056-8719(98)00027-6
3. L.A. Harris, J.D. Goff, A.Y. Carmichael, J.S. Riffle, J.J. Harburn, Chem. Mater. **15**, 1367 (2003). doi:10.1021/cm020994n
4. M. Vallet-Regí, J.C. Doadrio, A.L. Doadrio, I. Izquierdo-Barba, J. Pérez-Pariente, Solid State Ionics **172**, 435–439 (2004)
5. P. Horcajada, A. Rámila, J. Pérez-Pariente, M. Vallet-Regí, Microporous Mesoporous Mater. **68**, 105–109 (2004)
6. I. Izquierdo-Barba, L. Ruiz-González, J.C. Doadrio, J.M. González-Calbet, M. Vallet-Regí, Solid State Sci. **7**, 983–989 (2005). doi:10.1016/j.solidstatesciences.2005.04.003
7. A. Sousa, E.M.B. Sousa, J. Non-Cryst. Solids **352**, 3451 (2006). doi:10.1016/j.jnoncrysol.2006.03.080
8. A.L. Doadrio, E.M.B. Sousa, J.C. Doadrio, J.P. Pariente, I. Izquierdo-Barba, M. Vallet-Regi, J. Control Release **97**, 125 (2004). doi:10.1016/j.jconrel.2004.03.005
9. K.C. Souza, G. Salazar-Alvarez, J.D. Ardisson, W.A.A. Macedo, E.M.B. Sousa, Nanotechnology **19**, 561 (2008)
10. A. Sousa, K.C. Souza, E.M.B. Sousa, Acta Biomater. **4**, 671 (2008)
11. T. Sugimoto, E. Matijevic, J. Colloid Interface Sci. **74**, 227 (1979). doi:10.1016/0021-9797(80)90187-3
12. J.-S. Choi, S.-S. Yoon, S.-H. Jang, W.-S. Ahn, Catal. Today **111**, 280 (2006). doi:10.1016/j.cattod.2005.10.037
13. D. Zhao, J. Feng, Q. Huo, N. Melosh, G.H. Fredrickson, B.F. Chmelka, G.D. Stucky, Science **279**, 548 (1998). doi:10.1126/science.279.5350.548
14. L.C.M. Pinto, (Quantikov – Um Analisador Microestrutural para o Ambiente WindowsTM), PhD Thesis, Universidade de São Paulo- USP, Instituto de Pesquisas Energéticas e Nucleares – IPEN, 1996
15. J.A. Ritter, A.D. Ebner, K.D. Daniel, K.L. Stewart, J. Magn. Magn. Mater. **280**, 184 (2004). doi:10.1016/j.jmmm.2004.03.012
16. T. Higuchi, J. Pharm. Sci. **50**, 874 (1961). doi:10.1002/jps.2600501018
17. P. Costa, J.M.S. Lobo, Eur. J. Pharm. Sci. **13**, 123 (2001). doi:10.1016/S0928-0987(01)00095-1
18. N.A. Peppas, Pharm. Acta Helv. **60**, 110 (1985)
19. P.L. Ritger, N.A. Peppas, J. Control. Release **5**, 23 (1987). doi:10.1016/0168-3659(87)90034-4